

TiO₂ nanotube array film prepared by anodization as anode material for lithium ion batteries

Zhen Wei · Zheng Liu · Rongrong Jiang ·
Chaoqing Bian · Tao Huang · Aishui Yu

Received: 22 April 2009 / Revised: 22 July 2009 / Accepted: 28 July 2009 / Published online: 20 August 2009
© Springer-Verlag 2009

Abstract TiO₂ array film fabricated by potentiostatic anodization of titanium is characterized by X-ray diffraction (XRD), scanning electron microscopy (SEM), and charge–discharge measurements. The XRD results indicated that the TiO₂ array is amorphous, and after calcination at 500°C, it has the anatase form. The pore size and wall thickness of TiO₂ nanotube arrays synthesized at different anodization voltages are highly dependent on the applied voltage. The electrochemical performance of the prepared TiO₂ nanotube array as an electrode material for lithium batteries was evaluated by galvanostatic charge–discharge measurement. The sample prepared at 20 V shows good cyclability but low discharge capacity of 180 mA h cm⁻³, while the sample prepared at 80 V has the highest discharge capacity of 340 mA h cm⁻³.

Keywords TiO₂ nanotube · TiO₂ array film · Anodization · Lithium ion intercalation

Introduction

The worldwide thirst for portable consumer electronics in recent years has had an enormous impact on portable power. The performance advantages of lithium ion batteries are much better than those of other choices in the secondary battery market. For the emerging applications, fundamental studies with regard to specific energy, safety, cyclic stability, and cost are much needed. For example, graphite

is commonly used in commercial Li-ion batteries, but its operating voltage is too close to Li electroplating voltage to form a solid electrolyte interface (SEI layer), raising concerns over safety and loss of capacity [1, 2].

TiO₂ has a small volume expansion ratio (3%) [3] of intercalation/extraction of Li ions, good cyclic stability [2], and high discharge voltage plateau (about 1.7 V), so TiO₂ is an excellent candidate employed as a stable electrode in lithium ion batteries. Well-oriented TiO₂ nanotubes offer a large internal surface area without a concomitant decrease in structure order and excellent pathways for Li-ions to transfer between interfaces.

Anodic oxidation is a good method to fabricate highly ordered vertically oriented TiO₂ array film. In 2001, Grimes et al. [4] prepared uniformly ordered TiO₂ nanotube arrays by anodic oxidation method using HF solution as electrolyte and pure Ti sheet as substrate for the first time, which led to the upsurge of research on TiO₂ nanotube arrays. So far, lots of attention has been paid to the electrochemical properties of the TiO₂ nanotubes [5], nanoribbons [6], and nanowires [7] prepared by hydrothermal method, anodic aluminum oxide (AAO) template method, and electrodeposition method; however, electrochemical properties of TiO₂ array films prepared by anodic oxidation have not been investigated yet. Our purpose is to evaluate the electrochemical characteristics of the TiO₂ array films fabricated by anodic oxidation approach.

Experimental

Material preparation

Pure titanium sheet was purchased from Baoji Jucheng Titanium Industry Co., Ltd; and the other chemicals were

Z. Wei · Z. Liu · R. Jiang · C. Bian · T. Huang · A. Yu (✉)
Department of Chemistry, Shanghai Key Laboratory of Molecular
Catalysis and Innovative Materials, Institute of New Energy,
Fudan University,
Shanghai 200433, China
e-mail: asyu@fudan.edu.cn

purchased from Shanghai Chemical Co., Ltd. All chemicals were used as received without any further purification.

TiO₂ array film was prepared by potentiostatic anodization of the titanium sheet. Before anodizing experiments, the titanium sheet, with a thickness of 0.3 mm, was cleaned in deionised water, degreased in acetone and ethanol for 30 min, respectively, and then rinsed with 0.5 mol L⁻¹ sodium hydroxide solution and 30% (wt%) hydrogen peroxide with a volume ratio of 1:1 to remove the titanium oxide layer. After washing with deionised water, the pretreated Ti sheet was dried in air. The anodizing experiments were carried out using Ti sheet as both working and counter electrodes, with 1.0% (wt.%) NH₄F ethylene glycol solution as electrolyte. The anodized voltage was selected as 20, 40, 60, 80, and 100 V, and anodized time was fixed at 20 h. After the anodizing experiment, the resulting sheet was rinsed with deionised water, and then calcined in a muffle furnace at 500 °C.

Characterization and electrochemical measurements

The powder X-ray diffraction (XRD) patterns were measured on a Bruker D8 Advance X-ray diffractometer using Cu K α radiation. The morphologies were characterized using scanning electron microscopy (SEM) (JEOL JEM-2010).

The electrochemical performance of as-prepared TiO₂ array film was evaluated using a swagelok cell, in which TiO₂ array film sheet was used as working electrode and lithium metal as counter electrode, and the electrolyte used was 1 M LiPF₆ dissolved in a mixed solvent of ethylene carbonate (EC) and dimethyl carbonate (DMC) (1:1 in weight). The cells were assembled in an argon-filled glove box at room temperature, and all the electrochemical charge–discharge measurements were carried out in the voltage range of 1.0–2.7 V at 0.1 mA.

Results and discussion

Characteristics of samples

The XRD patterns of TiO₂ nanotube arrays are shown in Fig. 1. All the samples prepared under different potentials are amorphous before calcinations, and the typical XRD prepared at 60 V is given in Fig. 1a as an example. It can be seen from Fig. 1a that, before calcination, all the peaks could be ascribed to substrate Ti and no peaks for TiO₂ were observed. After calcinations at 500 °C for 4 h, besides the peaks for the substrate Ti, all diffraction peaks can be indexed as anatase TiO₂ (ICDD-JCPDS Card No. 89-4921). The peak at about 25.3° is typical for the crystal face (101) reflection of the anatase TiO₂. When calcinations occur at 500 °C for 8 h (Fig. 1c), the intensity of peaks for anatase TiO₂ is improved, indicating that the TiO₂ film is well

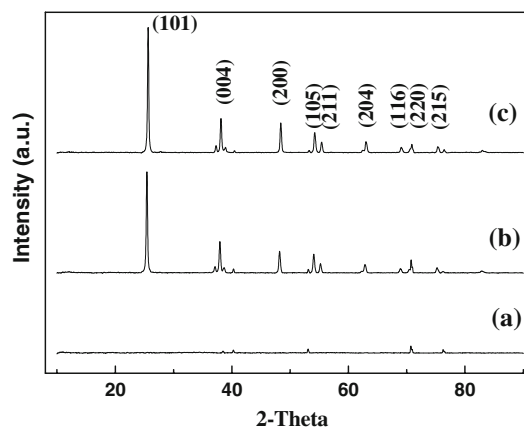


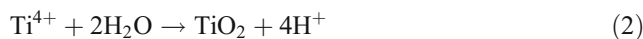
Fig. 1 XRD patterns of TiO₂ nanotube arrays prepared at 60 V and calcinated at 500 °C for different times: **a** before calcinations, **b** 4 h, **c** 8 h

crystallized, which means longer calcination time leading to better crystallization. In this study, all the tests are based on the samples calcined at 500 °C for 8 h.

Figure 2 shows the SEM images of the TiO₂ nanotube array films at different anodization voltages. Even at a relatively low voltage of 20 V, TiO₂ nanotubes with uniform pore size were formed; however, those arrays were not in a well-ordered orientation. The samples prepared at higher voltages of 40, 60, and 80 V consisted of highly ordered, well-oriented TiO₂ nanotubes. The average pore size increased from 50 (±10), to 100 (±10), to 150 (±10) nm and wall thickness from 25 (±5), to 40 (±5), to 50 (±5) nm, with the anodization voltage increasing from 20, to 40, to 60 V. The average pore size and wall thickness of 80 V are almost the same as those of 60 V; however, at the voltage of 80 V, the top of the sample began to be eroded. With further increases in anodization voltage to 100 V, the nanotubes collapsed.

The relationship between pore diameter, wall thickness, and anodization voltage is shown in Fig. 3. The reason for this relationship is related to a complicated procedure of formation of TiO₂ nanotube array at the titanium foil surface. The mechanism of nanotube array formation is as follows [8]:

1. In a very early stage, a barrier layer of compact titania is formed due to interaction of the metal with O²⁻ or OH⁻ ions in the effect of the electric field [9]



2. Fluorine ions near the anode react with TiO₂ with the help of the electric field, and the resultant TiF₆²⁻

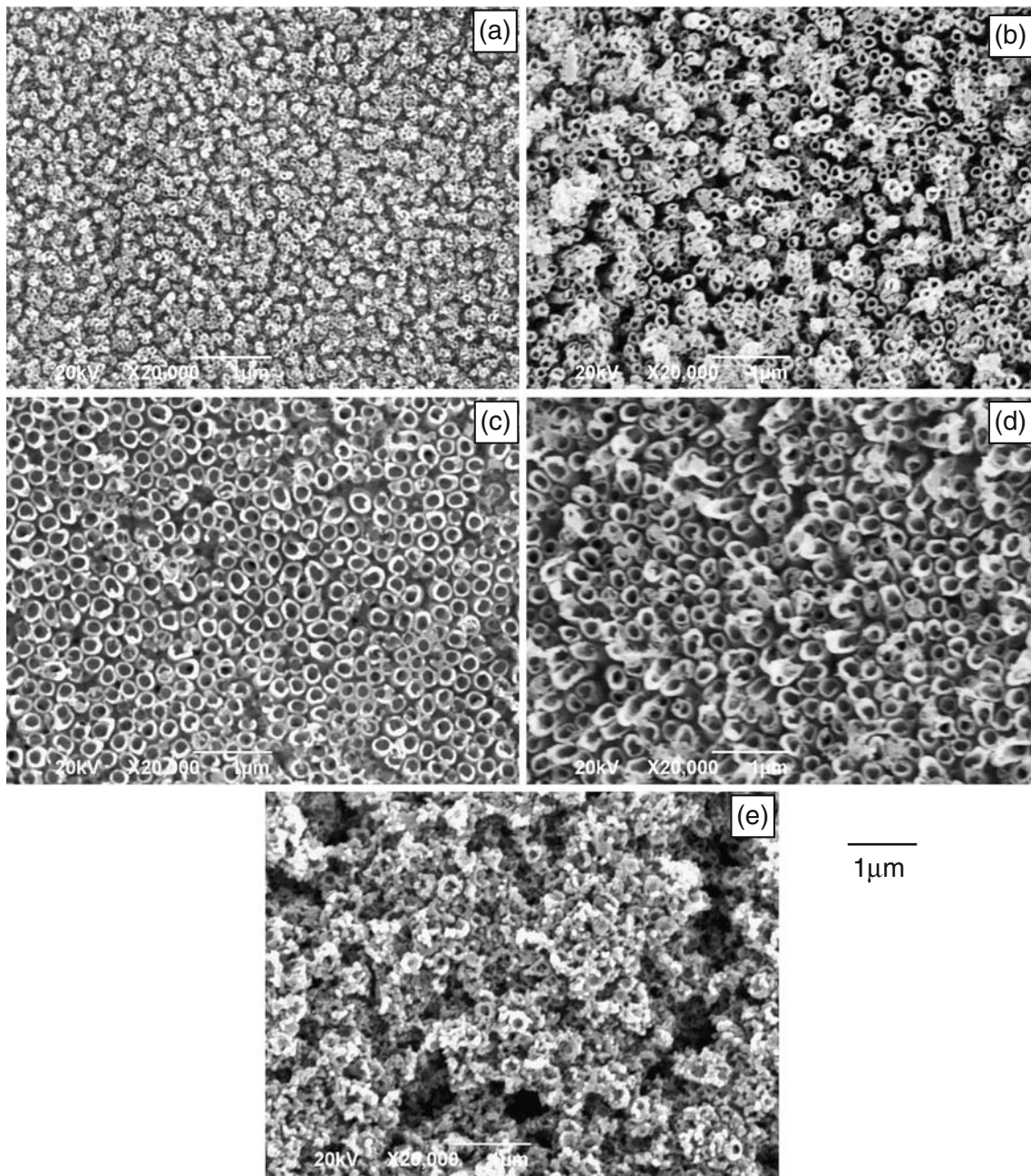
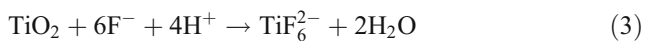


Fig. 2 SEM images of TiO₂ nanotube arrays fabricated in different anodization voltages: **a** 20 V, **b** 40 V, **c** 60 V, **d** 80 V, **e** 100 V

dissolved in water, which introduces cracks on the metal surface.



3. These cracks convert into bigger pores and the pore density increases. After that, the pores spread uniformly over the surface.

4. When the rate of oxide growth at the metal/oxide interface and the rate of oxide dissolution at the oxide/electrolyte interface finally become equal, the thickness of the barrier layer remains unchanged, although it moves further into the metal with the pore growing longer.
5. The nanotube length increases until the electrochemical oxidation rate equals the chemical dissolution rate of the top surface of the nanotubes. A completely self-organized porous layer is obtained.

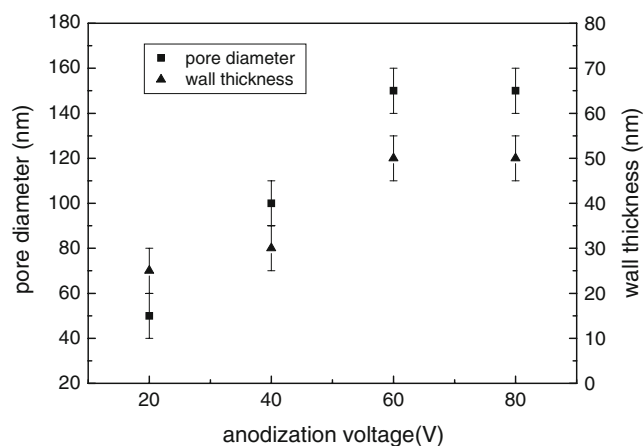


Fig. 3 Pore diameters and wall thicknesses of TiO₂ nanotube arrays fabricated in different anodization voltages

The curves in Fig. 3 indicate that the higher anodization voltage results in the bigger pore diameter and higher wall thickness. This can be understood within the context of procedure 3. The electric field distribution in the curved bottom surface of the pore causes pore widening, as well as deepening of the pore [10]. So, with a higher anodization potential, it is reasonable that the pore diameter is bigger; meanwhile, more current is distributed in the pore, which restrains other cracks from converting into pores, so pore density is lower and the nanotube wall is thicker with a higher anodization potential.

The collapse of nanotubes can be understood by procedures 2 and 3. TiO₂ at the metal surface is eroded by fluorine ions, which causes cracks. The cracks convert into bigger pores in the presence of electric field. So at a very high voltage, the pore sizes increase too fast to connect with each other, with some parts of the nanotube walls being completely eroded, which leads to the collapse of the nanotubes. At the voltage of 80 V, the top of the sample has already begun to erode, which is a sign of the voltage being too high.

Electrochemical behavior of samples

Charge–discharge measurement was performed to examine the electrochemical behavior of the TiO₂ film as a lithium interaction electrode, and its voltage–capacity profiles are presented in Fig. 4. For all the samples, the discharge plateau of the curve is flat at around 1.7 V vs Li/Li⁺. Figure 4a shows the initial capacities of TiO₂ nanotubes fabricated at different anodization voltages. The sample prepared under the voltage of 20 V has the initial discharge capacity of 180 mA hcm⁻³. As the anodization voltage increased to 40 V, the initial discharge capacity

increased to 270 mA hcm⁻³. Further increased voltage can also lead to the increase of the initial discharge capacity, which is 320 and 340 mA hcm⁻³ at the voltages of 60 and 80 V.

Although the sample of 20 V has a low specific energy, its reversibility is excellent, with the capacity retention of 96.4% for the first 140 cycles. With the increasing voltage, the fading of the capacity accelerates. For the samples prepared at the voltage of 40 V, the capacity retention of the first 140 cycles is 53.0%. And when the anodization voltages are up to 60 and 80 V, the capacity retentions are as low as 37.1% and 43.5%, respectively. The reason for this could be attributed to the pore size differences with different anodization voltages.

The sample of 20 V has a low capacity, which indicates that its utilization of active materials is low. The reason could be that TiO₂ nanotubes are a bit narrow and not straight and it is not easy for lithium ions to reach the very depth of the film. Since only the surface of the film can be utilized, its cyclic stability is very good. By increasing the applied voltage, the pore diameter grows bigger and straighter, so it becomes easier for lithium ions to get into the bottom of the film, and the resulting capacity increases. However, the TiO₂ nanotube array fabricated at high potential (80 and 100 V) is not stable enough to maintain its structure during lithium intercalation/deintercalation process, which results in poor cyclability.

It is well known that one significant disadvantage of TiO₂ is the poor lithium ionic and electronic conductivity of bulk TiO₂ polymorphs. This property can be well improved by making TiO₂ into nanotube arrays, in which the Li-diffusion length is reduced in the solid phase so the specific capability increases due to more active materials being utilized [2, 11, 12]. Nanopore structure provides a short path for Li⁺ transportation, which allows materials with low ionic conductivity to be applied in the battery [13, 14].

It is worth mentioning that the densities of samples are really difficult to measure. The nanotubes grow firmly on the substrate, and the inherent structure will be changed if they are scratched off the substrate. Porosity rate of the sample fabricated at a high potential is much larger than that fabricated at a low potential. Actually, the densities of all samples are lower than those of common particulate anatase TiO₂. Thus, the capacity unit has to be selected as mA hcm⁻³.

Conclusions

A well-ordered, vertically oriented TiO₂ nanotube array has been successfully fabricated by potentiostatic

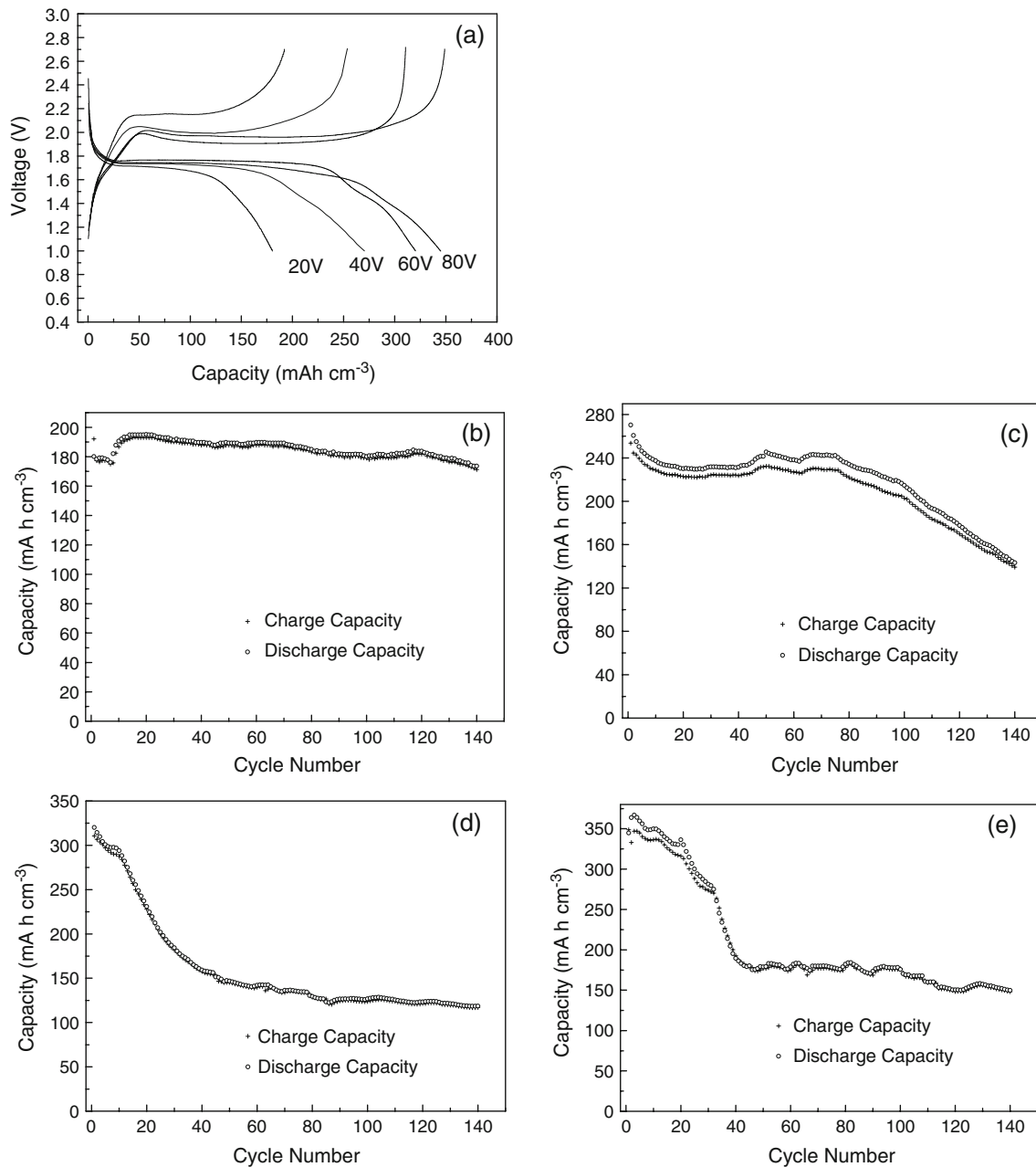


Fig. 4 Electrochemical performance of TiO_2 nanotube arrays. Initial capacities for TiO_2 nanotubes fabricated at different anodization voltages (a) and capacities for the first 140 cycles at 20 V (b), 40 V (c), 60 V (d), and 80 V (e)

anodization with different pore sizes and wall thicknesses. The XRD studies reveal that the TiO_2 array is amorphous, and after calcinations at 500°C , the amorphous TiO_2 turns to anatase form. The SEM results indicate that, at a low anodization voltage of 20 V, nanotubes just begin to form, but not in an oriented way. However, at a very high anodization voltage of 100 V, TiO_2 nanotube arrays were collapsed. The preferred voltage range for TiO_2 nanotube array film could be from 40 to 80 V in our preparation conditions.

The as-prepared TiO_2 array films showed good electrochemical behavior for lithium intercalation. The sample prepared at a voltage of 20 V gives a capacity of 180 mA h cm^{-3} with excellent cyclic stability. This synthesis procedure could be applied to prepare electrode materials for 3D batteries.

Acknowledgements This work is financially supported by Science & Technology Commission of Shanghai Municipality (08DZ2270500) and National “973” Project (No. 2009CB220100).

References

1. Croce F, Appetecchi GB, Persi L, Scrosati B (1998) *Nature* 394:456
2. Wang DH, Choi DW, Yang ZG, Viswanathan VV, Nie ZM, Song YJ, Zhang JG, Liu J (2008) *Chem Mater* 20:3435
3. Wagemaker M, Kearley GJ, van Well AA, Mutka H, Mulder FM (2003) *J Am Chem Soc* 125:840
4. Wang YQ, Hu GQ, Duan XF, Sun HL, Xue QK (2002) *Chem Phys Lett* 365:427
5. Yuan ZY, Colomer JF, Su BL (2002) *Chem Phys Lett* 363:362
6. Zhang XY, Yao BD, Zhao LX, Liang CH, Zhang LD, Mao YQ (2001) *J Electrochem Soc* 148:G398
7. Gong D, Grimes CA, Varghese OK, Gong D, Grimes CA, Varghese OK, Hu W, Singh RS, Chen Z, Dickey EC (2001) *J Mater Res* 16:3331
8. Sun L, Li J, Zhuang HF, Lai YK, Wang CL, Lin CJ (2007) *Chinese J Inorg Chem* 23:1841
9. Parkhutik VP, Shershulsky VI (1992) *J Phys D: Appl Phys* 25:1258
10. Gopal KM, Oommen KV, Maggie P, Karthik S, Craig AG (2006) *Sol Energy Mater Sol Cells* 90:2011
11. Maier J (2005) *Nat Mater* 4:805
12. Wang Y, Cao GZ (2006) *Chem Mater* 18:2787
13. Attia A, Zukalova M, Rathousky J, Zukal A, Kavan L (2005) *J Solid State Electrochem* 9:138
14. Moriguchi I, Hidaka R, Yamada H, Kudo T (2005) *Solid State Ionics* 176:2361